International Journal of Surface Science and Engineering

ISSN online: 1749-7868 - ISSN print: 1749-785X
https://www.inderscience.com/ijsurfse

Studying the load capacity and frictional force in an engine based on microtexture's different dimensions

Jili Zha, Vanliem Nguyen

DOI: 10.1504/IJSURFSE.2024.10065740

Article History:

Received:	28 March 2024
Last revised:	01 May 2024
Accepted:	10 May 2024
Published online:	04 March 2025

Studying the load capacity and frictional force in an engine based on microtexture's different dimensions

Jili Zha and Vanliem Nguyen*

School of Mechanical and Electrical Engineering,
Hubei Key Laboratory of Intelligent Conveying Technology and Device,
Hubei Polytechnic University,
Huangshi, 435003, China
Email: zhajili.hbpu@gmail.com
Email: xuanliem712@gmail.com
*Corresponding author

Abstract: The solid contact force (F_{sc}) and frictional force (F_{fsc}) generated in the mixed lubricating zone of the crank pin bearing are very high and greatly affect the engine power. Based on the lubricating model of the crank pin bearing, the hemispherical structure (HS) and round cylindrical structure (RCS) of the microtextures are researched and added in this mixed lubricating zone to reduce both F_{sc} and F_{fsc}. Research indicates that both HS and RCS improve the lubrication and friction better than without microtextures (WMT). Besides, HS's performance in improving the lubrication and friction is also better than RCS. Especially, with the optimised HS using r_t = 1.4 mm and h_t = 10 μm, the average values of F_{sc} and F_{fsc} are reduced by 35.1% and 36.4% compared to HS while these average values are greatly reduced by 56.9% and 57.4% compared to WMT. Therefore, this is a feasibility study in improving engine power.

Keywords: engine power; crank pin bearings; load capacity; frictional force; microtextures; hemispherical structure; round cylindrical structure; RCS.

Reference to this paper should be made as follows: Zha, J. and Nguyen, V. (2025) 'Studying the load capacity and frictional force in an engine based on microtexture's different dimensions', *Int. J. Surface Science and Engineering*, Vol. 19, No. 1, pp.43–60.

Biographical notes: Jili Zha is an Associate Professor Dr. at the School of Mechanical and Electrical Engineering, Hubei Polytechnic University. His current research interests include vehicle and mechanical dynamics, optimal design, engineering materials, and microstructure.

Vanliem Nguyen is a doctor and works at School of Mechanical and Electrical Engineering, Hubei Polytechnic University. His current research interests include vehicle dynamics, vibration and optimisation control, and lubrication in the engine.

1 Introduction

Improving friction, lubrication, and wear of journal bearings to enhance their working efficiency has been researched and developed (Nonogaki and Nakahara, 2006; Amanov et al., 2016). With the journal bearings that rotate at high speeds and are subject to stable loads, the lubrication characteristics of the sliding/non-slip surface pair in these journal bearings mainly occur the hydrodynamic lubrication (i.e., minimum lubricating oil film greater than 10 μm). Accordingly, both friction and load-capacity in journal bearing are mainly created by both shear stress and pressure in the oil generated in gap of the journal bearing (Bayada and Meurisse, 2009; Dwivedi et al., 2013). In order to ameliorate the lubricating efficiency in this journal bearing, the design parameters of the shaft and bearing as well as the parameters of the oil film were analysed and optimised (Tauviqirrahman et al., 2013; Ma et al., 2021). Thus, the journal bearing's lubricating efficiency has been significantly ameliorated. However, studies also show that to increase the lubricating capacity, concurrently, reduce frictions generated of the journal bearing, the minimum value of the film thickness in journal bearing's clearance needs to be increased. It means that the gap between the shaft and bearing needs to be increased. Therefore, this can increase the impaction between two surfaces of the shaft and bearing, resulting in the journal bearing's durability can decrease rapidly. This is a problem that is difficult to solve solely based on the journal bearing's design parameters. Accordingly, based on the development of laser technology in designing the different structures of the microtextures (Aizawa et al., 2019; Li et al., 2023), the microtextures have been investigated on surfaces of journal bearing to enhance minimum thickness of the lubricating oil film. Research results show that the journal bearing's lubrication has been significantly improved compared to ignoring microtextures (Maan and Awasthi, 2021; Shisode et al., 2021; Ibrahim et al., 2022; Yang et al., 2023).

With journal bearings that rotate at high speeds and are subject to large loads that change over cycles, such as the crank pin bearings in the internal combustion engine, the lubrication of these journal bearings is very complicated because the lubrication flow in these journal bearings is not guaranteed. Accordingly, in the lubrication process of the crank pin bearings, two different lubrication zones have appeared including the hydrodynamic lubrication (i.e., minimum lubricating oil film greater than 10 μm) and mixed lubrication (i.e., minimum lubricating oil film smaller than 10 μm) (Mourelatos, 2001; Guzzomi et al., 2008; Gregory and Katia, 2011; Lia et al., 2016; Zhao et al., 2016). In this mixed lubricating zone, the solid contacts created by the rough bearing surface and rough shaft surface have happened. Therefore, both friction and loading capacity in crank pin bearing are not only determined by the shear stress and pressure of the lubricating oil film in the hydrodynamic lubrication zone, but it also depends greatly on the shear stress and pressure generated by solid contacts between two surfaces of journal bearing at mixed lubricating zone (Zhao et al., 2016; Zhang et al., 2016; Nguyen et al., 2021a). To improve the lubricating efficiency of this crank pin bearing, the solid contacts in the mixed lubricating zone of the crank pin bearing need to be reduced. This means that the frictional force and load capacity generated by solid contacts in the mixed lubricating zone of the crank pin bearing should be reduced. Therefore, the design parameters of the crank pin bearing in the engine have been analysed and optimised to reduce these solid contacts (Lia et al., 2016; Ma et al., 2021; Xu et al., 2021). Research shows that to reduce these solid contacts, the surface roughness of the bearing and crank pin needs to be minimised. This is a difficult problem to solve when machining the bearing and crank pin

surfaces. However, increasing the minimum thickness in oil film can reduce area of mixed lubricatinal zone, thereby reducing the solid contact force and frictional force generated by the solid contacts in the mixed lubricating zone of the journal bearing. Thus, the crank pin bearing's lubrication can be improved.

Based on lubrication studies of the journal bearings adding microtextures to increase the minimum lubricating oil film thickness, different structures of microtextures including hemispherical structures, wedge-shaped structures, round cylindrical structures (RCS), square cylindrical structures, triangular structures, and mixed structures have been studied and evaluated for their effectiveness in improving the journal bearing's lubrication (Gropper et al., 2016; Xu et al., 2021; Arif et al., 2021; Wang et al., 2022). The results show that hemispherical structures and RCS can better improve the journal bearing's lubrication compared to other structures proposed. Accordingly, these two types of structures can also be applied and designed to the mixed lubricating zone of the crank pin bearing to increase the minimum lubricating oil film thickness as well as improve the engine's frictional force and load capacity.

In this investigation, based on the lubrication dynamic model of the engine's crank pin bearing, two different types of microtextures using the hemispherical structures and RCS are added in the mixed lubricating zone of the crank pin bearing to improve the engine's friction and loading capacity. Influence of various parameters including the distribution densities and geometric dimensions in designed textures on loading capacity and friction in an engine are then simulated and analysed to optimise their efficiency. Reducing solid-contact forces as well as reducing frictional forces in solid contact area of the crank pin bearing is the objective in this paper.

Main contributions of this investigation includes:

1 Based on the lubricating model of the crank pin bearing, the hemispherical structure and RCS of the microtextures are researched and added in this mixed lubricating zone to reduce the solid contact force and frictional force generated in the mixed lubricating zone of the crank pin bearing.

2 Influences in various parameters of microtextures on both load capacity and frictional forces of an engine are fully analysed to optimise their efficiency.

3 Research has found that the hemispherical structure of microtextures with optimal parameters greatly improves the lubricating capacity and frictional force of the engine.

2 Model and calculation method

2.1 Lubricational dynamic model of engine's crank pin bearing

During the working process of the internal combustion engine, under the effect of the air pressure generated in the engine's fuel combustion process, the impacting force (F) of the connecting rod crankshaft mechanism that always changes in intensity and direction then acts on the crank pin bearing. Accordingly, to ensure lubrication for the crank pin bearing, the load capacity (F_0) generated by the oil film must be balanced with the impacting force of F ($F = F_0$). However, during rotation of the crank pin bearing, the frictional force (F_f) of the crank pin bearing is also generated, thus, $F_0 < F$, and the

engine's power is significantly reduced. Especially, at the engine's combustion-power cycle corresponding to the crankshaft rotation angle from 2π to 2.3π rad, both values of F_0 and F_f reach the largest value while the minimum lubricating oil film thickness is smaller than 10 µm. This is the mixed lubricating zone of the crank pin bearing (Zhao et al., 2016; Nguyen et al., 2021a), as shown in Figure 1. Accordingly, this mixed lubricating zone needs to be researched to ameliorate the lubricational ability and frictional force in the engine's crank pin bearing.

Figure 1 Model of an engine's crank pin bearing with the characteristics of the cylinder pressure and crank pin bearing's load capacity and frictional force (see online version for colours)

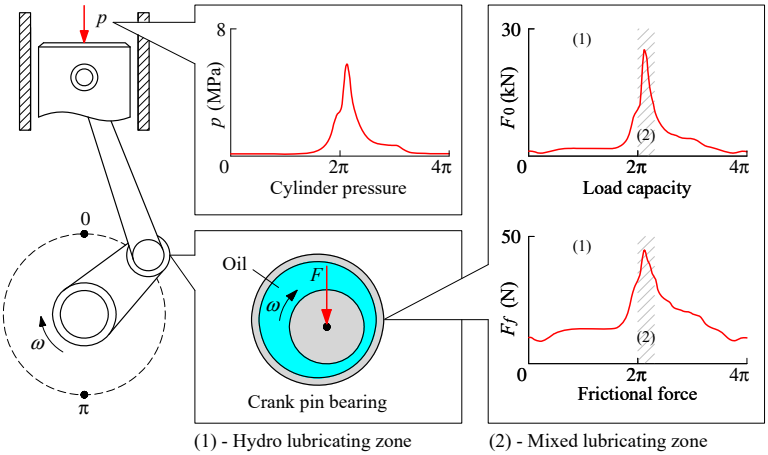

Under the impaction of force F from the connecting rod crankshaft mechanism acting on the crank pin bearing when the engine's crankshaft is rotating at a velocity of ω, the centre of the bearing with radius r_b and the centre of the crank pin with radius r_c are misaligned by a very small distance e. Thus, the thickness of the oil film (h) is unevenly distributed in the crank pin bearing's clearance. Based on the hydro lubricating model of the engine's crank pin bearing (Gregory and Katia, 2011; Hua et al., 2022), a lubricational dynamic model of the crank pin bearing with its Cartesianism counterpart is established in Figure 2 to describe in detail the lubrication of the crank pin bearing. Herein, ϕ is the angular coordinate of the crank pin bearing from 0 to 2π rad ($\phi = 0$ at the maximum thickness of the oil film h_{oil}). ψ is the attitude angle of the crank pin bearing. p has been presented as pressure of oil film in crank pin bearing. $L_x = 2\pi r_b$ and $L_y = B$ are the length and width of the bearing. $u_0 = r_b\omega$ is the relative speed between two surfaces of bearing and shaft. l_1 and $(L_x - l_2)$ are the lengths of the hydro lubricating zone. $(l_2 - l_1) = Lx/4r_b$ is the length of the mixed lubricating zone.

Based on the calculation result of h in the lubricational models of the journal bearing and crank pin bearing, the h in Figure 2 can be expressed by (Zhao et al., 2016; Hua et al., 2022):

$$h = (\varepsilon \cos\phi + 1)c \tag{1}$$

Herein $\varepsilon = e/c$ is defined as the eccentricity ratio between two centres of crank pin and bearing, $c = r_b - r_c$.

Figure 2 Lubricational dynamic model of the crank pin bearing with its Cartesianism counterpart (see online version for colours)

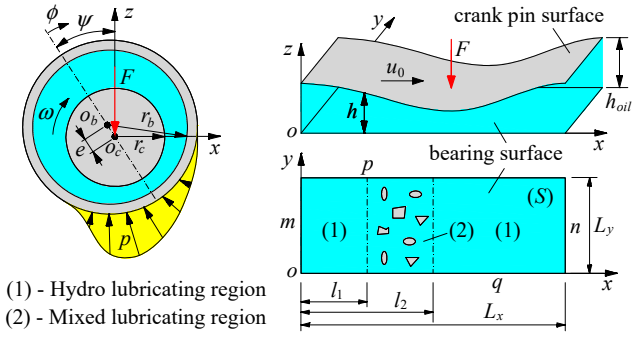

In order to compute the lubricational equation of the crank pin bearing in Figure 2, some assumptions of the lubricational model need to be made as follows:

1 The lubricating film in the gap of crank pin bearings always exists, the viscosity and density of the lubricating film are constant during the crank pin bearing rotating, and the inertia of the lubricating film is negligible when the lubricating film moving.

2 The bearing's surface does not move at all the x, y, and z directions.

Crank pin is rotated at a speed of u_0 in the x direction, thus, the lubricating film's speed in the y and z directions is zero. Besides, the lubricating film's speed of bearing is also zero at x direction and lubricating film's speed at the crank pin surface is u_0 in the x direction.

Additionally, the journal bearing's existing research showed that the rough bearing surface and rough shaft surface greatly affect its lubrication and friction (Patir and Cheng, 1978; Wu and Zheng, 1989; Tauviqirrahman et al., 2013; Nguyen et al., 2021b). Therefore, two factors (φ_x and φ_y) of the pressure flow (Patir and Cheng, 1978) affected by the surface roughness of the crank pin bearing in x, y directions as well as shear factor (φ_s) of oil flow (Wu and Zheng, 1989) affected by the surface roughness of the crank pin bearing in the x direction are also added to fully research the lubrication of the crank pin bearing. From the lubricational dynamic model of the crank pin bearing plotted in Figure 2, the Reynolds equation used to calculate the motions of (p, h) in lubricating film of crank pin bearing is expressed as follows (Patir and Cheng, 1978; Wu and Zheng, 1989; Hua et al., 2022):

$$\frac{\partial}{\partial x}\left(h^3\varphi_x\frac{\partial p}{\partial x}\right)+\frac{\partial}{\partial y}\left(h^3\varphi_y\frac{\partial p}{\partial y}\right)=6\eta\left(u_0\frac{\partial h}{\partial x}+\sigma u_0\frac{\partial \varphi_s}{\partial x}+2\frac{\partial h}{\partial t}\right) \tag{2}$$

where σ is the height of the average roughness between two surfaces of the crank pin bearing and η is the oil film's viscosity, $\varphi_s = 1.126e^{-0.25\alpha}$ if $\alpha > 5.0$ and $\varphi_s = 1.899\alpha^{0.89e-0.92\alpha+0.05\alpha 2}$ if $\alpha \leq 5.0$, $\varphi_x = \varphi_y = 1–0.9e^{-0.56\alpha}$ (Patir and Cheng, 1978; Wu and Zheng, 1989).

Based on the constant parameters of the crank pin bearing including c, L_x, L_y, p_0, and t_0, the lubricational equation of the crank pin bearing in equation (2) can be written as follows:

$$\frac{\partial}{L_x\partial x/L_x}\left(c^3\frac{h^3}{c^3}\varphi_x\frac{p_0\partial p/p_0}{L_x\partial x/L_x}\right)+\frac{\partial}{L_y\partial y/L_y}\left(c^3\frac{h^3}{c^3}\varphi_y\frac{p_0\partial p/p_0}{L_y\partial y/L_y}\right)$$
$$=6\eta u_0\frac{c\partial h/c}{L_x\partial x/L_x}+6\eta u_0\sigma\frac{\partial\varphi_s}{L_x\partial x/L_x}+12\eta\frac{c\partial h/c}{t_0\partial t/t_0} \tag{3}$$

Or

$$\frac{L_y^2}{L_x^2}\frac{\partial}{\partial x/L_x}\left(\frac{h^3}{c^3}\varphi_x\frac{\partial p/p_0}{\partial x/L_x}\right)+\frac{\partial}{\partial y/L_y}\left(\frac{h^3}{c^3}\varphi_y\frac{\partial p/p_0}{\partial y/L_y}\right)=\frac{6\eta u_0L_y^2}{c^2L_xp_0}\frac{\partial h/c}{\partial x/L_x}$$
$$+\frac{6\eta u_0L_y^2\sigma}{c^3L_xp_0}\frac{\partial\varphi_s}{\partial x/L_x}+\frac{12\eta L_y^2}{c^2p_0t_0}\frac{\partial h/c}{\partial t/t_0} \tag{4}$$

Let $X = x/L_x$, $Y = y/L_y$, $P = p/p_0$, $\alpha = L_y/L_x$, $H = h/c$, $\Omega_1 = 6\eta u_0L_y^2/c^2L_xp_0$, $T = t/t_0$, $\Omega_2 = 6\eta u_0L_y^2/c^3L_xp_0$, $\Omega_3 = 12\eta L_y^2/c^2p_0t_0$ and $T = t/t_0$ Thus, equation (4) is then simply written as follows:

$$\alpha^2\frac{\partial}{\partial X}\left(\varphi_xH^3\frac{\partial P}{\partial X}\right)+\frac{\partial}{\partial Y}\left(\varphi_yH^3\frac{\partial P}{\partial Y}\right)=\Omega_1\frac{\partial H}{\partial X}+\Omega_2\frac{\partial\varphi_s}{\partial X}+\Omega_3\frac{\partial H}{\partial T} \tag{5}$$

Therefore, equation (5) has been described as the dimensionless equation of the crank pin bearing's lubricational dynamic model.

To simulate the lubricational equation in equation (5), some boundary conditions of the crank pin bearing's lubricational dynamic model in Figure 2 need to be defined as follows:

1 The maximum lubricational oil film of the crank pin bearing is the inlet oil film and outlet oil film at $\phi = 0$ of *m*-line and $\phi = 2\pi$ of *n*-line.

2 The lubricational calculation area of the crank pin bearing is *S*, the inlet pressure at *m*-line, outlet pressure at *n*-line, and the ambient pressures at *m*-, *n*-, *p*-, and *q*-lines of the calculation domain *S* (see Figure 2) are the atmospheric pressure of p_0.

Therefore, the *p* at four boundary lines of *S* is calculated by:

$$p\big|_{x=0}^{m\text{-line}} = p\big|_{x=Lx}^{n\text{-line}} = p \text{ and } p\big|_{y=0}^{q\text{-line}} = p\big|_{y=Ly}^{p\text{-line}} = 0 \tag{6}$$

Additionally, the lubricational process of the crank pin bearing can appear cavitation regions with the negative pressure of p_n. However, the lubricating equation of Reynolds in the model of journal bearings cannot calculate the cavitation pressure of p_n (Braun and Hannon, 2010; Wang et al., 2011). In order to compute the pressure of the lubricating film in cavitation regions, p_n generated at cavitation regions is replaced by the saturation pressure of p_s as follows (Braun and Hannon, 2010):

$$p_n = p \text{ with } p_s \le p \text{ and } p_n = p_s \text{ with } p_s > p \tag{7}$$

By combining equations (5)–(7), all the pressure of the lubricating film in the lubricational calculation area of the crank pin bearing can be determined.

2.2 Model of crank pin bearing added by microtextures of HS and RCS

In order to ameliorate the load capacity as well as decrease the frictional force in the engine's crank pin bearing, both the solid contact force and frictional force in the mixed lubricating zone of the crank pin bearing need to be reduced. This means that the minimum thickness of the lubricating film in the mixed lubricating zone needs to be increased. Therefore, at the mixed lubricating zone of the crank pin bearing surface, two different types of microtextures using the hemispherical structures (HS) and RCS are proposed as well as supported to enhance minimum thickness of the lubricating film, as plotted in Figure 3. Where a and b are the distribution densities of microtextures at x, y direction. l_x and l_y are the distance between two consecutive microtextures at x, y direction. r_t and h_t are radius and depth of each microtexture of the HS or RCS. Thus, the dimension relationship between the bearing surface and HS or RCS can be calculated by $L_x = (2r_t + l_x)a$ and $L_y = (2r_t + l_y)b$.

Figure 3 Model of two different structures of microtextures added on the surface of the bearing in the crank pin bearing's mixed lubricating zone (see online version for colours)

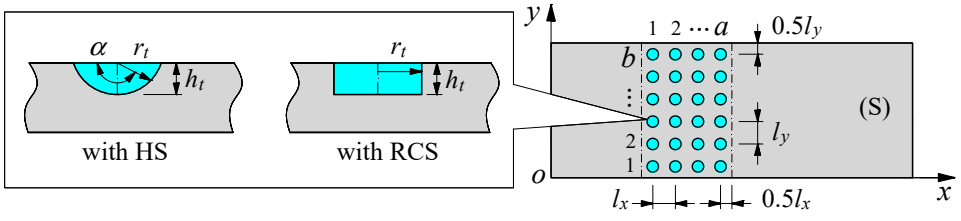

From the structure of the HS and RCS added on the surface of the bearing in the crank pin bearing's mixed lubricating zone, the thickness of the lubricating film in equation (1) with HS and RCS is expressed by:

$$h = \begin{cases} c(\varepsilon\cos\phi + 1) - \dfrac{\cos\alpha - 1}{\sin\alpha} r_t & \text{with HS} \\ c(\varepsilon\cos\phi + 1) + h_t & \text{with RCS} \end{cases} \tag{8}$$

Besides, the distribution equations of the HS and RCS on the bearing surface also need to be calculated. Thus, based on the design of the HS and RCS, the distribution equation of each HS or RCS (x_i and y_j) at its circle centre at x, y direction has been calculated as:

With HS:

$$r_t \geq \sqrt{(x - x_i)^2 + (y - y_j)^2} \text{ and } \frac{1 - \cos\alpha}{\sin\alpha} h_t \geq z \geq 0 \tag{9}$$

With RCS:

$$r_t \geq \sqrt{(x - x_i)^2 + (y - y_j)^2} \text{ and } z = h_t \tag{10}$$

where $x_i = \left(i - \dfrac{1}{2}\right)\dfrac{L_x}{a}$ with $i = 1, 2, 3, \ldots, a$ and $y_j = \left(j - \dfrac{1}{2}\right)\dfrac{L_y}{b}$ with $j = 1, 2, 3, \ldots, b$.

By combining equations (8)–(10), the value of h with the HS and RCS as well as the distribution of the HS and RCS can be determined to calculate the lubrication of the crank pin bearing.

2.3 Method for evaluating the load capacity and friction of crank pin bearing

2.3.1 Load capacity of crank pin bearing

Under the impacting force of F on the crank pin bearing, two different lubrication zones of the crank pin bearings including hydrodynamic lubrication and mixed lubrication have appeared (Akalin and Newaz, 2001; Zhao et al., 2016; Maan and Awasthi, 2021). Accordingly, to ensure lubrication for the crank pin bearing, the load capacity in crank pin bearings (F_0) calculated based on load capacity in oil film (F_{lf}) at the hydrodynamic lubrication zone and load capacity in solid contact (F_{sc}) at mixed lubricating zone must be balanced with the F. The calculation formulas of F_0, F_{lf}, and F_{sc} are expressed by (Wang et al., 2011; Hua et al., 2022):

$$F_0 = F_{lf} + F_{sc} = F \tag{11}$$

$$F_{lf} = \sqrt{\left(-\iint_S p \sin\phi dxdy\right)^2 + \left(-\iint_S p \cos\phi dxdy\right)^2} \tag{12}$$

$$F_{sc} = \sqrt{\left(-\iint_S p_{sc} \sin\phi dxdy\right)^2 + \left(-\iint_S p_{sc} \cos\phi dxdy\right)^2} \tag{13}$$

Herein p has been calculated in equations (5)–(7). p_{sc} is the pressure of the solid contact in the mixed lubricating zone of the crank pin bearing.

The rough surfaces of the bearing and shaft were mainly created based on Gaussian distribution and it was described by Greenwood and Tripp (1970):

$$p_{sc} = 1.5\pi\lambda^2 E^* \sqrt{\sigma/\zeta} \prod \text{with} \begin{cases} \prod = 4.4086\times10^{-5}(4-h/\sigma)^{6.804} & \text{if } h/\sigma < 4 \\ \prod = 0 & \text{if } h/\sigma \geq 4 \end{cases} \tag{14}$$

Herein $\lambda = \eta\sigma\zeta$, ζ is the curvature radius of the solid roughness, Π is solid roughness's probability in crank pin bearing's surfaces, and E^* is material's elasticity modulus.

2.3.2 Frictional force of crank pin bearing

Similarly, in the slipping process between the crank pin surface and bearing surface, the frictional force (F_f) of the crank pin bearing is also determined based on the frictional force of the lubricating film (F_{flf}) in the hydrodynamic lubrication zone and the frictional force of the solid contact (F_{fsc}) in the mixed lubricating zone. The calculation formulas of F_f, F_{flf}, and F_{fsc} are expressed by (Patir and Cheng, 1978; Zhao et al., 2016):

$$F_f = F_{lf} + F_{fsc} \tag{15}$$

$$F_{flf} = \iint_S \tau_{lf} dxdy \tag{16}$$

$$F_{fsc} = \iint_S \tau_{sc} dxdy = \iint_S \left(\tau_0 + p_{sc}\mu_0\right) dxdy \tag{17}$$

where τ_{lf} is the shear stress of the lubricating film, τ_{sc} is the shear stress of the solid contact in the mixed lubricating zone, μ_0 and τ_0 are the frictional coefficient and shear stress at the bearing boundaries.

2.3.3 Objective investigations

As described in equations (11) and (15), load capacity as well as friction (F_0, F_f) in crank pin bearings depend on the lubricating film's load capacities and frictions (F_{lf}, F_{flf}) and load capacities and friction (F_{sc}, F_{fsc}) at solid contacts in crank pin bearing's mixed lubricating zone. Both F_{of} and F_{fof} of the lubricating film in the hydro lubricating zone have been researched and evaluated (Gregory and Katia, 2011; Zhao et al., 2016; Nguyen et al., 2021b). However, both F_{sc} and F_{fsc} of solid contacts in the mixed lubricating zone of the crank pin bearing have not been evaluated in detail, especially both F_{sc} and F_{fsc} in the mixed lubricating zone added by microtextures of HS and RCS. Therefore, to evaluate the load capacity and frictional force in the engine's crank pin bearing under different structures and dimensions of microtextures, both F_{sc} and F_{fsc} in the mixed lubricating zone of the crank pin bearing described in equations (13) and (17) are chosen as the evaluation indexes.

3 Numerical simulation results and discussions

3.1 Lubricational and frictional performance between HS and RSC

From the design parameters and lubricational parameters of the engine's crank pin bearing given at Table 1 (Guzzomi et al., 2008; Hua et al., 2022), impact force of the connecting rod crankshaft mechanism on the crank pin bearing at ω = 2,000 rpm in Figure 4 (this impact force calculated from the experimental data of the air pressure in the engine's fuel combustion process in the existing studies (Zhao et al., 2016; Nguyen et al., 2021b), and HS and RCS's initial parameters provided in the same Table 1, the computation programs written in MATLAB environment is applied to compute the lubricating equations in equations (5)–(10) and the values of F_{sc} and F_{fsc} in equations (13) and (17).

Table 1 Designed parameters of the crank pin bearing and microtextures

Parameters of crank pin bearing				*Parameters of HS and RCS*			
Parameters	*Values*	*Parameters*	*Values*	*Parameters*	*Values*	*Parameters*	*Values*
$B\ (m)$	20×10^{-3}	$\eta\ (Pas)$	0.02	$L_x\ (m)$	$50\pi \times 10^{-3}$	$\alpha\ (rad)$	$0–\pi$
$r_b\ (m)$	25×10^{-3}	$E\ (GPa)$	140	$L_y\ (m)$	20×10^{-3}	a	4
$c\ (m)$	10×10^{-6}	$\phi\ (rad)$	$0–4\pi$	$h_t\ (m)$	6.0×10^{-6}	b	6
$\sigma\ (m)$	4×10^{-6}	$\tau_0\ (N/m^2)$	2.00×10^6	$r_t\ (m)$	0.8×10^{-3}	p_0 (Pa)	101,325

Figure 4 The impact force of the connecting rod crankshaft mechanism on the crank pin bearing at ω = 2,000 rpm

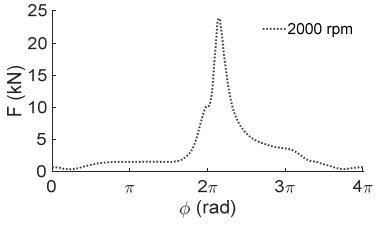

Figure 5 Bearing surface added by the HS and RCS with the distribution densities of a = 4 and b = 6: (a) with HS, (b) with RCS (see online version for colours)

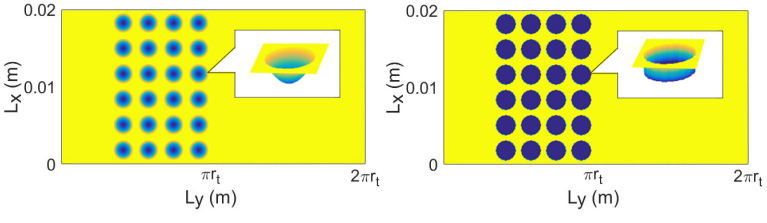

Figure 6 Calculation results of the crank pin bearing added by the HS and RCS with a = 4 and b = 6: (a) thickness of the lubricating film (h), (b) pressure of the lubricating film (p), (c) load capacity of solid contacts (F_{sc}), (d) frictional force (F_{fsc}) of solid contacts in the crank pin bearing (see online version for colours)

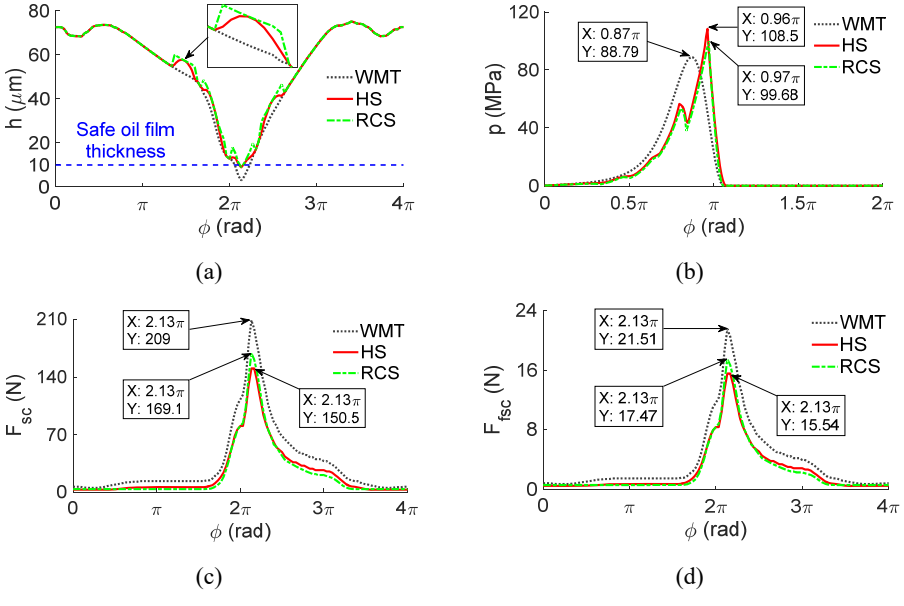

Based on the microtextures of the HS and RCS with the distribution densities of $a = 4$ and $b = 6$ added on the surface of the bearing at the crank pin bearing's mixed lubricating zone, the distribution results of the HS and RCS on the bearing surface are simulated and plotted in Figures 5(a) and 5(b). From the distribution data of HS and RCS in Figure 5, the h, pressure (p), the load capacity at solid contacts (F_{sc}), and the frictional force (F_{fsc}) of solid contacts are computed and presented in Figures 6(a)–6(d).

With case of bearing surface without microtextures (WMT), Figure 6(a) shows that the lubricating film's minimum thickness (minimum $h < 10$ μm) occurs in a range ϕ from 2π to 2.3π (this is the crank pin bearing's mixed lubricating zone). Due to the influence of the increase of solid contacts in the crank pin bearing's mixed lubricating zone, thus, the p of the lubricating film is reduced and the pressure p_{sc} of solid contacts is increased. Thus, both the F_{sc} and F_{fsc} in the solid contact zone are quite high. As shown in Figures 6(b)–6(d), maximum value p only reaches 88.79 MPa while both the maximum values of F_{sc} and F_{fsc} are achieved at 209N and 21.51N.

By adding the HS or RCS with the distribution densities of $a = 4$ and $b = 6$ on the surface of the bearing at the mixed lubricating zone to reduce solid contacts of the crank pin bearing, Figure 6(a) shows that the minimum h with the HS and RCS in mixed lubricating zone of the crank pin bearing is increased with the minimum $h \geq 10$ μm. This implies that solid contacts of crank pin bearing surfaces are significantly reduced. Accordingly, the p of the oil film is increased. Based on the calculation equations (10) and (15), when the p is increased, this means the lubricating film's load capacity is creased and load capacity of the solid contact is reduced (the pressure p_{ac} of the solid contact is reduced). With the p reduced, this means that the shear stress generated by the solid contacts is also reduced. As a result, both the F_{sc} and F_{fsc} generated in the mixed lubricating zone are reduced. As shown in Figures 6(b)–6(d), results of p with the HS and RCS is higher than that of the WMT while the results of F_{sc} and F_{fsc} with the HS and RCS is lower than that of the WMT. The maximum p with the HS and RCS is achieved at 108.5 MPa and 99.68 MPa while both the maximum values of F_{sc} and F_{fsc} with the HS and RCS are achieved at {169.1N and 150.5N} and {17.47N and 15.54N}. This is the performance of the microtextures designed on the sliding/non-slip surface pair of the journal bearing to ameliorate both the lubricating capacity and frictional force (Ma et al., 2021; Shisode et al., 2021; Arif et al., 2021; Wang et al., 2022).

Besides, the comparison results between the HS and RCS in the same Figure 6 also show that although the radius (r_t) and maximum depth (h_t) between the HS and RCS are the same [see Figure 6(a) and Table 1], however, the maximum p with the HS is higher than the maximum p with the RCS. It implies that the pressure of solid contacts (p_{sc}) of the HS is lower than that of the RCS, thus, the maximum F_{sc} and maximum F_{fsc} of the HS are also lower than that of the RCS, as shown in the same Figures 6(b)–6(d). This may be due to the influence of the different structures between the HS and RCS. With the HS, the depth of h_t is changed slowly and reaches its maximum value at $h_t = 6.0 \times 10^{-6}$ m, thus, the appeared cavitation region in the HS is reduced and the maximum p of the lubricating film with the HS is increased. On the contrary, with the RCS, the depth of $h_t = 6.0 \times 10^{-6}$ m is unchanged, thus, the appeared cavitation region in the RCS is more than in the HS and the maximum p with the RCS is smaller than that of the HS. This has been explained in the existing studies (Wang et al., 2011; Xu et al., 2021). As a result, load capacity as well as friction in tmixed lubricating zone with RCS are higher than those of the HS.

Figure 7 The maximum value of the F_{sc} and F_{fsc}: (a) maximum F_{sc}, (b) maximum F_{fsc} (see online version for colours)

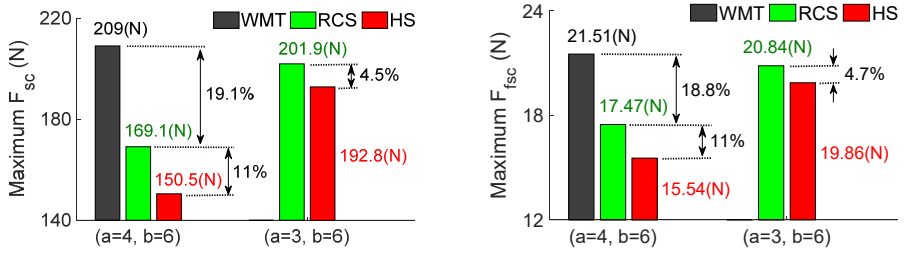

(a) (b)

From the comparison results of the maximum F_{sc} and maximum F_{fsc} with the HS and RCS designed by their distribution densities of $a = 4$ and $b = 6$ in Figure 7, we can see that the maximum F_{sc} and maximum F_{fsc} with the RCS are reduced by 19.1% and 18.8% compared to the WMT while the maximum F_{sc} and maximum F_{fsc} with the HS are lower than that of the RSC by 10.9% and 11.0%. This means that both the HS and RCS improve the lubricational and frictional performance of the engine's crank pin bearing better than the WMT. Besides, the performance of the HS is also better than the RCS. However, this result is compared under the distribution densities of the HS and RCS with $a = 4$ and $b = 6$. This may not fully reflect the performance between HS and RCS.

Figure 8 Calculation results of the crank pin bearing added by the HS and RCS with $a = 3$ and $b = 6$: (a) with HS, (b) with RCS, (c) result of F_{sc}, (d) result of F_{fsc} (see online version for colours)

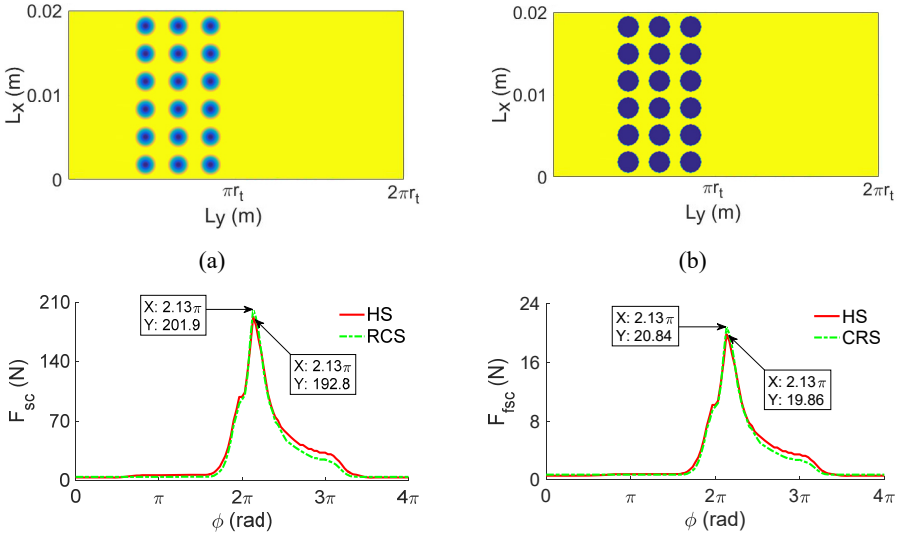

(a) (b)

(c) (d)

Therefore, other distribution densities of the HS and RCS with $a = 3$ and $b = 6$ are also simulated to more fully evaluate the performance between HS and RCS. The distribution results of the HS and RCS with $a = 3$ and $b = 6$ designed on bearing of the crank pin

bearing are plotted in Figures 8(a) and 8(b). From these distribution densities, both the F_{sc} and F_{fsc} are computed in Figures 8(c) and 8(d). The result also shows that the maximum F_{sc} and maximum F_{fsc} with the HS are also lower than that of the RCS. The maximum F_{sc} and maximum F_{fsc} of the HS are reduced by 4.5% and 4.7% compared to the RCS (see Figure 7 with $a = 3$ and $b = 6$). This means that with the distribution results of the HS and RCS with $a = 3$ and $b = 6$ designed, the HS also improves the lubricational and frictional performance of the engine's crank pin bearing better than the RCS. Besides, the comparison results in Figure 7 also show that the distribution densities of the HS and RCS also affect the lubricational and frictional performance of the crank pin bearing. Both the maximum F_{sc} and maximum F_{fsc} of the HS and RCS with $a = 3$ and $b = 6$ are greatly increased compared to the HS and RCS with $a = 4$ and $b = 6$. This is because the reduced density of the HS or RCS can increase solid contacts between the crank pin surface and bearing surface in the mixed lubricating zone, therefore, both F_{sc} and F_{fsc} are increased.

From the above analysis results, it can be concluded that the HS with $a = 4$ and $b = 6$ improves the lubricational and frictional performance of the engine's crank pin bearing better than the RCS with $a = 3$, 4, and $b = 6$. However, the research result also shows that solid contacts in the crank pin bearing's mixed lubricating zone depend on the solid contact density or radius r_t of the HS. To optimise the HS's performance, the radius r_t (solid contact density) of the HS with $a = 4$ and $b = 6$ continues to be researched in Section 3.2.

3.2 Load capacity and frictional force of solid contact under the change of HS's radius

Under the same simulation condition of the crank pin bearing in Section 3.1, a change range of the HS's radius from r_t = [0.2, 0.3, 0.4, …, 1.5, 1.6] mm is then simulated to assess the effect of r_t on the HS's performance. The results of the force characteristics of F_{sc} and F_{fsc} under the change of r_t are shown in Figures 9(a) and 9(b). Besides, the average values of F_{sc} and F_{fsc} at each changed value of r_t are computed and plotted in Figures 9(c) and 9(d).

Figures 9(a) and 9(b) show that the change of r_t mainly affects the maximum F_{sc} and maximum F_{fsc} of the crank pin bearing. When the r_t is reduced, the solid contacts in the crank pin bearing's mixed lubricating zone are increased. This means that both the p_{sc} and shear stress of the solid contacts are strongly increased. Concurrently, the area of solid contacts between bearing surface and crank pin surface is also increased. Thus, both maximum F_{sc} and maximum F_{fsc} are increased and vice versa. To optimise the HS's performance, both F_{sc} and F_{fsc} should be reduced. Both Figures 9(c) and 9(d) present that average values of F_{sc} and F_{fsc} reach the minimum value at $r_t = 1.4$ mm. This means that this value should be chosen for designing the HS on the surface of the bearing to ameliorate the lubricational and frictional performance of the engine's crank pin bearing.

The HS is designed based on two basic parameters of the radius r_t and depth h_t. The research result shows that the HS's performance is greatly affected by the radius r_t. Thus, the HS's performance can be also affected by the depth h_t. To clarify this issue, the change of the h_t is also researched in Section 3.3.

Figure 9 Characteristic of F_{sc} and F_{fsc} under the change of HS's radius: (a) value of F_{sc}, (b) value of F_{fsc}, (c) average value of F_{sc}, (d) average value of F_{fsc} (see online version for colours)

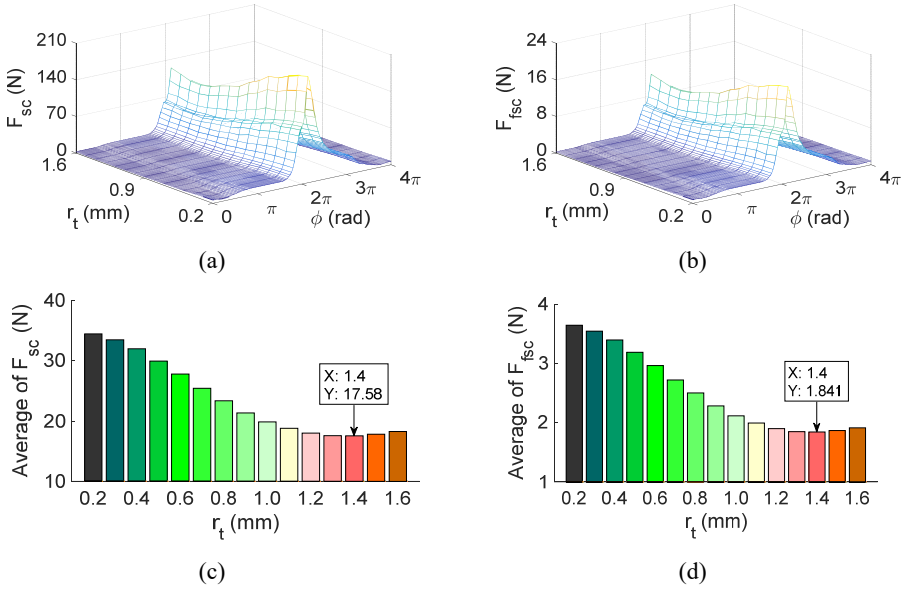

3.3 Load capacity and frictional force of solid contact under the change of HS's depth

Similarly, under the same simulation parameters of the crank pin bearing in Table 1 and the optimal radius of r_t = 1.4 mm in Section 3.2 used, a change range of the HS's depth from h_t = [2, 4, 6, …, 22, 24] μm is then simulated to assess the effect of h_t on the HS's performance. The simulation results of the force characteristics of F_{sc} and F_{fsc} are shown in Figures 10(a) and 10(b). Besides, the average values of F_{sc} and F_{fsc} at each change value of h_t are also computed and plotted in Figures 10(c) and 10(d).

Figures 10(a) and 10(b) show that the h_t mainly affects the maximum F_{sc} and maximum F_{fsc} in the mixed lubricating zone of the crank pin bearing when the h_t is changed in a range of $2 \leq h_t \leq 13$ μm. In this change range, both the maximum F_{sc} and maximum F_{fsc} are strongly reduced when the depth of h_t is increased. This is because the HS's lubricating film is increased, thereby reducing the solid contacts in the crank pin bearing's mixed lubricating zone. However, when the h_t is increased from 13 μm to 24 μm, both the maximum F_{sc} and maximum F_{fsc} are insignificantly reduced while both the values of F_{sc} and F_{fsc} in the hydro lubricating zone are quickly increased. This is due to the h_t being increased, h in HS has been increased and the cavitation region is also increased, thus, the p is reduced. To ensure the load capacity of the crank pin bearing, the p_{ac} is increased. As a result, both F_{sc} and F_{fsc} in the hydro lubricating zone are increased. In this change range, the h_t insignificantly improves the HS's performance. Based on the average values of F_{sc} and F_{fsc} computed in Figures 10(c) and 10(d), we can see that both these average values achieve minimum value at h_t = 10 μm. The optimal value of h_t in the existing study showed that the optimal value of ht should be used in a range from 10 to 18 μm (Zhao et al., 2016). Therefore, this research result is similar and this is the optimal value that can best improve the HS's performance.

Figure 10 Characteristic of the F_{fsc} and F_{fsc} under the change of HS's depth: (a) value of F_{fsc}, (b) value of F_{fsc}, (c) average value of F_{fsc},, (d) average value of F_{fsc} (see online version for colours)

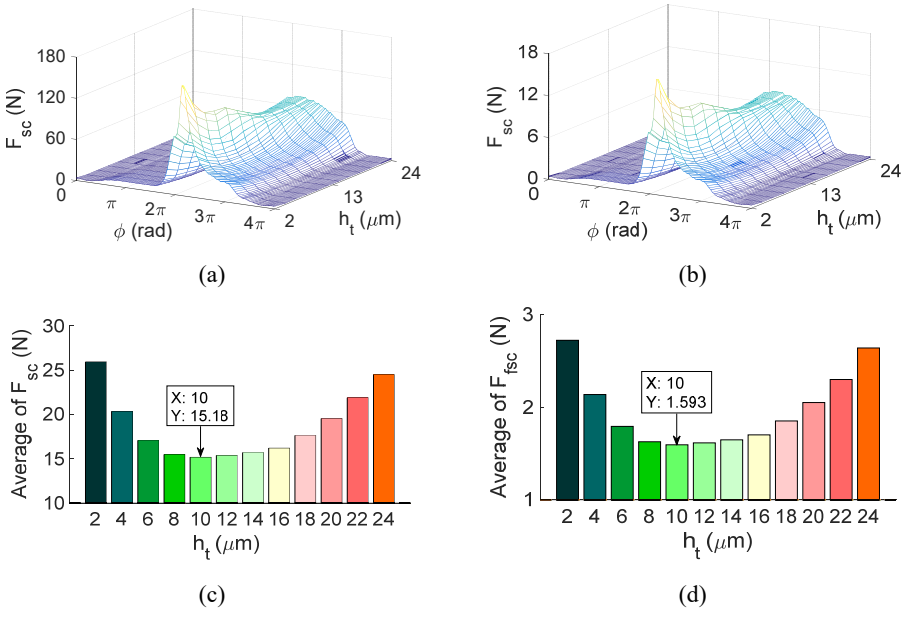

Figure 11 Result of F_{sc} and F_{fsc} with optimised HS (OHS): (a) value of F_{sc}, (b) value of F_{fsc}, (c) average value of F_{sc}, (d) average value of F_{fsc} (see online version for colours)

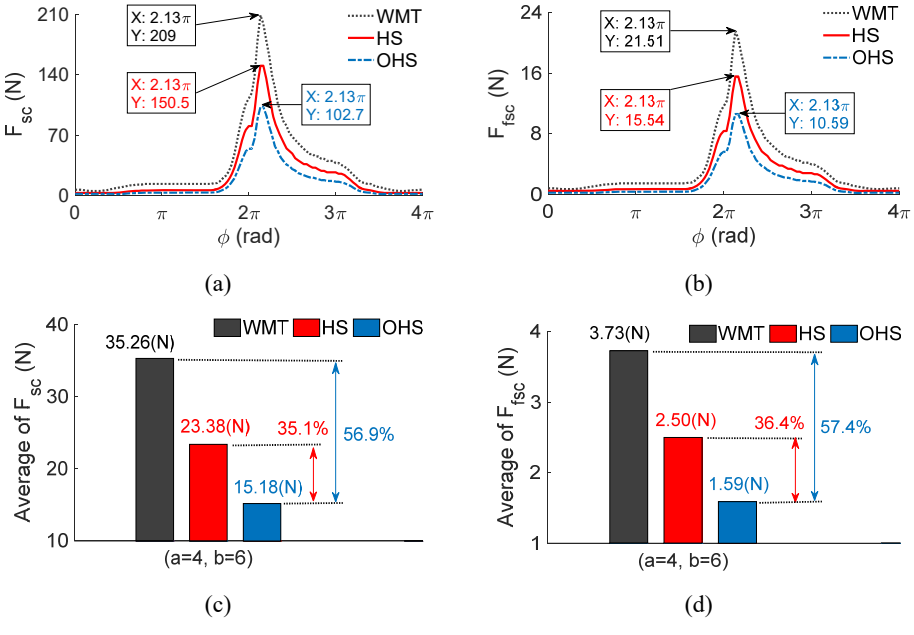

To evaluate the performance of the optimised HS (OHS) with the distribution densities of $a = 4$ and $b = 6$, the optimal parameters of $r_t = 1.4$ mm and $h_t = 10$ μm of the OHS are then simulated and compared with the HS and WMT. The results of F_{sc} and F_{fsc} and their average values are plotted in Figures 11(a)–11(d). Results in force characteristics of F_{sc} and F_{fsc} with the OHS are strongly reduced compared to both the HS and WMT. Especially, the average values of F_{sc} and F_{fsc} with the OHS are reduced by 35.1% and 36.4% in comparison with the HS while these average values with the OHS are greatly reduced by 56.9% and 57.4% compared to the WMT. Therefore, by using the OHS designed on bearing at the crank pin bearing's mixed lubricating zone, the lubricational and frictional performances of the engine's crank pin bearing are greatly improved in comparison with the WMT.

4 Conclusions

Under the same simulation condition of the engine, the HS and RCS added on the surface of the bearing in the crank pin bearing's mixed lubricating zone better improve the engine's lubricational and frictional performance in comparison with the WMT. Besides, the HS also improves the engine's lubricational and frictional performance better than the RCS.

Based on the design parameters of the radius and depth of the HS simulated, both these parameters greatly affect the HS's performance. To obtain the optimal HS's performance, the optimal parameters of $r_t = 1.4$ mm and $h_t = 10$ μm should be used for the design of the HS.

With the optimised HS using $r_t = 1.4$ mm and $h_t = 10$ μm, the average values of F_{sc} and F_{fsc} with the OHS are reduced by 35.1% and 36.4% in comparison with the HS while these average values with the OHS are greatly reduced by 56.9% and 57.4% compared to the WMT. Therefore, based on the results of this study and combined with laser technology in the design of microtextures on material surfaces, the OHS designed on the surface of the bearing in the mixed lubricating zone of the crank pin bearing not only greatly improves the engine's lubricational and frictional performance but also can be implemented in the actual condition.

This is highly applicable research in ameliorating the lubricating capacity and frictional force of the engine. In the next study, an experimental study of the crank pin bearing added by the OHS will be performed. In addition, the engine loads under different speeds will also be studied to evaluate the overall and detailed performance of the OHS.

References

Aizawa, T., Inohara, T. and Wasa, K. (2019) 'Femtosecond laser micro-/nano-texturing of stainless steels for surface property control', *Micromachines (Basel)*, Vol. 10, No. 8, p.512.

Akalin, O. and Newaz, G. (2001) 'Piston ring-cylinder bore friction modeling in mixed lubrication regime: part I – analytical results', *Journal of Tribology*, Vol. 123, No. 1, pp.211–218.

Amanov, A., Ahn, B., Lee, M., Jeon, Y. and Pyun, Y. (2016) 'Friction and wear reduction of eccentric journal bearing made of Sn-based babbitt for ore cone crusher', *Materials (Basel)*, Vol. 9, No. 11, p.950.

Arif, M., Kango, S. and Shukla, D. (2021) 'Investigating the effect of different slip zone locations on the lubrication performance of textured journal bearings', *Industrial Lubrication and Tribology*, Vol. 73, No. 6, pp.872–881.

Bayada, G. and Meurisse, M. (2009) 'Impact of the cavitation model on the theoretical performance of heterogeneous slip/no-slip engineered contacts in hydrodynamic conditions', *Proc. Inst. Mech. Eng. Part D: Journal of Engineering Tribology*, Vol. 223, No. 3, pp.371–381.

Braun, M. and Hannon, W. (2010) 'Cavitation formation and modelling for fluid film bearings: a review', *Proc. Inst. Mech. Eng. Part J: Journal of Engineering Tribology*, Vol. 224, No. 9, pp.839–863.

Dwivedi, V., Chand, S. and Pandey, K. (2013) 'Effect of number and size of recess on the performance of hybrid (hydrostatic/hydrodynamic) journal bearing', *Procedia Engineering*, Vol. 51, pp.810–817.

Greenwood, J. and Tripp, J. (1970) 'The contact of nominally flat rough surface', *Proceedings of the Institution of Mechanical Engineers*, Vol. 185, No. 1, pp.625–633.

Gregory, B. and Katia, L. (2011) 'Analysis of the dynamics of a slider-crank mechanism with hydrodynamic lubrication in the connecting rod-slider joint clearance', *Mechanism and Machine Theory*, Vol. 46, No. 10, pp.1434–1452.

Gropper, D., Wang, L. and Harvey, T. (2016) 'Hydrodynamic lubrication of textured surfaces: a review of modeling techniques and key findings', *Tribology International*, Vol. 94, pp.509–529, https://doi.org/10.1016/j.triboint.2015.10.009.

Guzzomi, A., Hesterman, D. and Stone, B. (2008) 'Variable inertia effects of an engine including piston friction and a crank or gudgeon pin offset', *Proc. Inst. Mech. Eng. Part D: Journal of Automobile Engineering*, Vol. 222, No. 3, pp.397–414.

Hua, W., Nguyen, V. and Jiao, R. (2022) 'Investigation of distribution and structure of surface textures on improving tribological properties of an engine', *SAE International Journal Engines*, Vol. 15, No. 3, pp.381–392.

Ibrahim, M., Ibrahim, M. and Hassan, A. (2022) 'Performance of non-metallic sliding element textured bearing', *International Journal of Surface Science and Engineering*, Vol. 16, No. 1, pp.1–16.

Li, G., Li, X., He, G., Fan, R., Li, F. and Ding, S. (2023) 'Surface quality and material removal rate in fabricating microtexture on tungsten carbide via femtosecond laser', *Micromachines (Basel)*, Vol. 14, No. 6, p.1143.

Lia, Y., Chen, G., Sun, D., Gao, Y. and Wang, K. (2016) 'Dynamic analysis and optimization design of a planar slider-crank mechanism with flexible components and two clearance joints', *Mechanism and Machine Theory*, Vol. 99, pp.37–57, https://doi.org/10.1016 /j.mechmachtheory.2015.11.018.

Ma, C., Liu, J., Zhu, X., Yan, Z., Cheng, D., Xue, W., Fu, J. and Ma, S. (2021) 'Optimization of surface texture fabricated by three-step microarc oxidation for self-lubricating composite coating of diesel engine piston skirts', *Wear*, Vols. 466–467, p.203557, https://doi.org/10.1016/j.wear.2020.203557.

Maan, J. and Awasthi, R. (2021) 'Effect of texture location on performance characteristics of two-lobe hydrodynamic journal bearing under turbulent regime', *Materials Today: Proceedings*, Vol. 47, No. 16, pp.5575–5583

Mourelatos, Z. (2001) 'An efficient journal bearing lubrication analysis for engine crankshafts', *Tribology Transactions*, Vol. 44, No. 3, pp.351–358.

Nguyen, V., Zhang, J. and Huang, D. (2021a) 'Influence of micro asperity contact and radial clearance on the tribological properties of crankpin bearings', *Journal of Southeast University*, Vol. 37, No. 3, pp.264–271.

Nguyen, V., Zhang, J., Jiao, R. and Huang, D. (2021b) 'Effects of crankpin bearing speed and dimension on engine power', *Journal of Southeast University*, Vol. 37, No. 2, pp.119–127.

Nonogaki, M. and Nakahara, T. (2006) 'Approximate formula for the contact between truncated surfaces and frictional characteristics of a journal bearing in mixed lubrication', *Lubrication Science*, Vol. 10, No. 3, pp.225–240.

Patir, N. and Cheng, H. (1978) 'An average flow model for determining effects of three-dimensional roughness on partial hydrodynamic lubrication', *Journal of Lubrication Technology*, Vol. 100, No. 1, pp.12–17.

Shisode, M., Hazrati, J., Mishra, T., Rooij, M. and Boogaard, T. (2021) 'Mixed lubrication friction model including surface texture effects for sheet metal forming', *Journal of Materials Processing Technology*, Vol. 291, p.117035, https://doi.org/10.1016/j.jmatprotec.2020.117035.

Tauviqirrahman, M. Ismail, R., Jamari, R., and Schipper, D. (2013) 'Optimization of the complex slip surface and its effect on the hydrodynamic performance of two-dimensional lubricated contacts', *Computers & Fluids*, Vol. 79, pp.27–43, https://doi.org/10.1016/j.compfluid.2013.02.021.

Wang, H., Ma, Y., Bai, Z., Liu, J., Huo, L. and Wang, Q. (2022) 'Evaluation of tribological performance for laser textured surfaces with diverse wettabilities under water/oil lubrication environments', *Colloids and Surfaces A: Physicochemical and Engineering Aspects*, Vol. 645, p.128949, https://doi.org/10.1016/j.colsurfa.2022.128949.

Wang, X., Zhang, J. and Dong, H. (2011) 'Analysis of bearing lubrication under dynamic loading considering micropolar and cavitating effects', *Tribology International*, Vol. 44, No. 9, pp.1071–1075.

Wu, C. and Zheng, L. (1989) 'An average Reynolds equation for partial film lubrication with a contact factor', *Tribology International*, Vol. 111, No. 1, pp.188–191.

Xu, S., Nguyen, V., Guo, X. and Yuan, H. (2021) 'Lubrication efficiency of crankpin bearing using square-cylindrical textures of partial textures optimized by genetic algorithm', *Industrial Lubrication and Tribology*, Vol. 73, No. 10, pp.1248–1257.

Yang, S. Song, Z., Tong, X. and Han, P. (2023) 'Study on the friction noise behaviour of coating textured surface based on STFT time-frequency analysis', *International Journal of Surface Science and Engineering*, Vol. 17, No. 4, pp.295–316.

Zhang, H., Hua, M., Dong, G., Dong, Z. and Chin, K. (2016) 'A mixed lubrication model for studying tribological behaviors of surface texturing', *Tribology International*, Vol. 93, No. B, pp.583–592.

Zhao, B., Dai, X., Zhang, Z. and Xie, Y. (2016) 'A new numerical method for piston dynamics and lubrication analysis', *Tribology International*, Vol. 94, pp.395–408, https://doi.org/10.1016/j.triboint.2015.09.037.

Zhao, B., Zhang, Z., Fang, C., Dai, X. and Xie, Y. (2016) 'Modeling and analysis of planar multibody system with mixed lubricated revolute joint', *Tribology International*, Vol. 98, pp.229–241, https://doi.org/10.1016/j.triboint.2016.02.024.